ISBN: 978-3-95450-201-1 doi:10.18429/JACoW-IBIC2018-WEPA16

MICROBUNCHING INSTABILITY MONITOR FOR X-RAY FREE ELECTRON LASER

C. Kim*, J.H. Ko, G. Kim, H.-S. Kang, and I.S. Ko
Pohang Accelerator Laboratory, POSTECH, Pohang 790-834, Korea

Abstract

A direct method was developed to measure the microbunching instability in the X-ray Free Electron Laser (XFEL). The microbunching instability comes from the interaction between the electron beam and the coherent synchrotron radiation (CSR), and the FEL intensity can be affected significantly by the microbunching instability. Until now, however, no effective method had been introduced to monitor the microbunching instability, and we tried to install a CCD camera to monitor the microbunching instability after the bunch compressor. The measurement result showed that the microbunching instability can be monitored by the CCD camera, and more interesting features of the microbunching instability were revealed from it.

INTRODUCTION

When an electron beam passes through an undulator, the spontaneous synchrotron radiation is generated and it can interact back with the electron beam again. The interaction makes the beam energy modulation on the scale of the resonant wavelength from the energy exchange between the radiation electric field and the oscillating motion of the electron beam to the transverse direction [1]. The undulator is a dispersive device and the energy modulation is changed into a longitudinal density modulation which is called a microbunching. The microbunching enhances the coherence of the radiation and increases the radiation intensity to develop a collective instability [2, 3]. The scale of the microbunching is much shorter than that of the bunch length and the microbunching instability grows up until the maximum bunching is achieved if the undulator length is long enough. In short, the microbunching instability is the working principle of Self-Amplified Spontaneous Emission (SASE) [4–6]

In the Free Electron Linac (FEL), bunch compressors are used to enhance the performance of the FEL by reducing the bunch length for high current and high brightness. A relativistic electron bunch can have an energy chirp while passing through the off crest of the linac RF phase before the bunch compressor, and lower energy electrons move to the front of the electron bunch and higher energy ones go back. Inside the bunch compressor, the electron beam passes through a strong dispersive section, and higher energy electrons follow a shorter trajectory and lower energy ones travel a longer trajectory. Because of the path length difference, the high energy electrons at the back of the electron bunch catch up with the lower energy ones in the front, and the bunch length decreases. In this process, it is important not

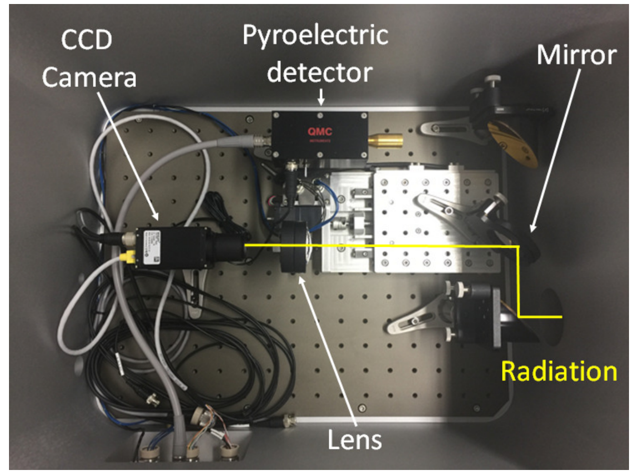

Figure 1: Experimental setup of the Coherent Radiation Monitor of PAL-XFEL.

to increase the energy spread or the transverse emittance beyond tolerances during the bunch compression.

Like an undulator, the bunch compressor is a dispersive device and synchrotron radiation can be generated from bending magnets. This means that the microbunching can be generated in the linac bunch compressor. Especially, Coherent Synchrotron Radiation (CSR) can be a source of the beam density modulation at wavelengths small compared to the bunch length. The effect of microbunching from CSR has been observed in computer simulations of the bunch compressor designed for the Linac Coherent Light Source (LCLS) [7], and in the bunch compressor simulation of the TESLA Test Facility [8]. Analytical studies of the CSR effects in bunch compressors also have been published in literature [9].

In this paper, we introduce a direct method to monitor the microbunching instability. A visible CCD camera is installed to measure the intensity of the coherent radiation after the bunch compressor. The measurement result shows that strong visible radiation is observed after the bunch compressor and the CCD camera can be used as a microbunching monitor without any beam interruption.

COHERENT RADIATION MONITOR

X-ray Free Electron Laser of Pohang Accelerator Laboratory (PAL-XFEL) is a hard X-ray FEL to produce 0.1 nm wavelength photon [10]. From a photo-cathode RF gun, an electron beam is generated with 5 MeV energy and 150 pC charge by using an Ultra-Violet (UV) laser pulse of 3 ps pulse width. The electron beam is accelerated to 10 GeV energy by using S-band (2856 MHz) RF structures in the

* chbkim@postech.ac.kr

ISBN: 978-3-95450-201-1 doi:10.18429/JACoW-IBIC2018-WEPA16

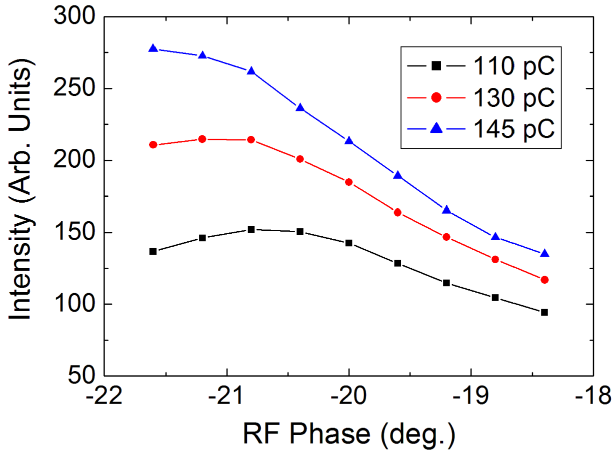

Figure 2: Intensity measurement results of the pyroelectric detector as a function of the linac RF phase before the second bunch compressor.

linac of which length is 780 m. In addition to acceleration, the electron bunch length is reduced down to 50 fs in full width at half maximum after two bunch compressors and 3 kA peak current is obtained at the linac end. The electron beam from the gun passes through two acceleration columns (L0) and reaches the energy of 130 MeV. The electron beam is accelerated to 0.36 GeV with the first linac section (L1) and the bunch length is compressed to 1.3 ps by using the first bunch compressor. After that, the electron beam is accelerated to 2.5 GeV energy with the second linac section (L2). The second linac is connected to the second bunch compressor and the bunch length is reduced to 50 fs. The fully compressed beam is accelerated to 10 GeV energy by using the rest of the linac. The electron beam comes into the undulator section after passing through a beam transport line and generates a hard X-ray pulse.

The intensity of the FEL radiation strongly depends on the bunch length with a given number of electron charges. Thus, the monitoring of the bunch length is a critical issue in the XFEL beam diagnostics. When the electron beam passes through the bunch compressor, radiation can be obtained after the bending magnet. Moreover, Coherent radiation can be obtained if the electron beam which emits the radiation is shorter than the radiation wavelength. After dipole magnets of the bunch compressor, the trajectory of the accelerated electron beam is bent and coherent synchrotron radiation (CSR) is generated. At the edge of the dipole magnet, the electron beam generates another coherent radiation which is called the coherent edge radiation (CER) [11]. Because the radiation intensity is inversely proportional to the bunch length, the bunch length can be estimated by measuring the radiation intensity. A coherent radiation monitor (CRM) is widely used after the bunch compressor for the bunch length monitoring [12]. The CRM shows the relative bunch length and a calibration is needed by using a transverse deflecting cavity which can measure the absolute bunch length.

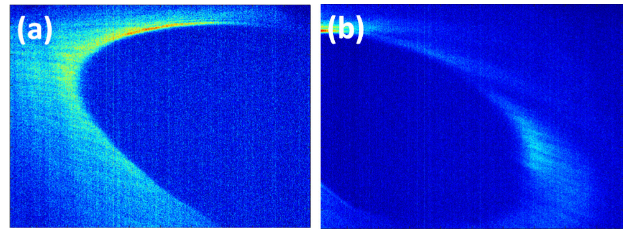

Figure 3: Images of the CCD camera when the mirror moves in the CRM chamber.

The experimental setup of the CRM is shown in Fig. 1. CSR and CER are reflected to a detector by using a gold-coated mirror with a center hole of 10 mm diameter for the electron bunch to pass through, and coherent diffraction radiation (CDR) can be generated when the electron beam passes through the mirror hole. Coherent radiation is guided into the low vacuum chamber by using the gold-coated mirror with a center hole. The low vacuum chamber is controlled under 10^{-1} torr of the air pressure and sealed with a CF-4.5-inch diamond window to reduce the attenuation of radiation intensity. In the low vacuum chamber, THz radiation is focused to a pyroelectric detector by using two parabolic mirrors. The parabolic mirror has 50.8 mm diameter and the gold-coated surface with more than 94% reflection from the terahertz to the visible range. The pyroelectric detector is installed in the focal point of the parabolic mirror to obtain the maximum signal strength. The pyroelectric detector measures the intensity of the terahertz radiation in the range from 0.1 THz to 20 THz and is suitable for the bunch length monitor considering 1.3 ps (= 0.77 THz) bunch length after the first bunch compressor.

MEASUREMENT RESULTS

After the second bunch compressor, the bunch length of the electron beam is reduced down to 50 fs (= 20 THz), which is twenty times shorter than the wavelength of the 1 THz, and the radiation becomes coherent one which makes saturation of the pyroelectric detector. In Fig. 2, the bunch length is increased as the L2 RF phase goes from $-22°$ to $-18°$. The L0 and the L1 phase are fixed to $0°$ and $-11°$, respectively. Note that the measurement result is saturated when the L2 phase is near to $-21°$.

We installed a visible CCD camera to measure the visible radiation intensity to avoid the saturation problem [13]. The nominal bunch length of 50 fs (= 15 μm) is longer than the visible wavelength (400 - 700 nm) and the electron beam energy (2.5 GeV) is high enough to generate the visible synchrotron radiation. The CCD camera setup consists of a moving stage, an aluminum coated mirror, and an uncoated focusing lens with a 50.8 mm diameter as shown in Fig. 1. To guide the visible radiation to the CCD camera, we moved the mirror on the moving stage and obtained the transverse image of visible coherent radiation. Figure 3a and 3b show images of the CCD camera as the mirror moves to the chamber wall in Fig. 1. The center hole boundary of

ISBN: 978-3-95450-201-1 doi:10.18429/JACoW-IBIC2018-WEPA16

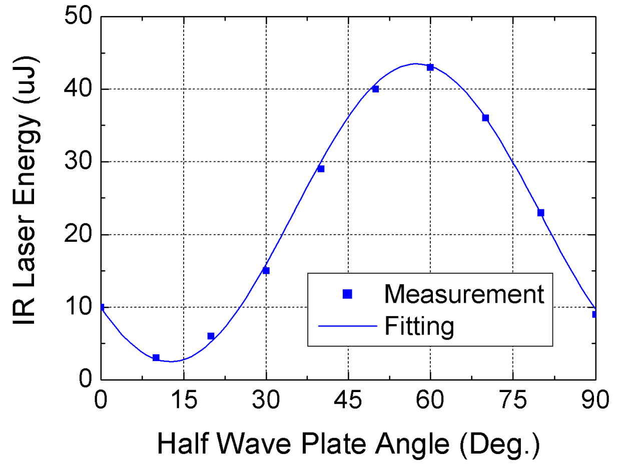

Figure 4: Half-wave-plate angle and IR laser energy relation of the laser heater.

the gold-coated mirror is clearly shown in the CCD camera image. An important thing was that the intensity of the visible radiation was surprisingly strong when the bunch length was near to the minimum.

In PAL-XFEL, a laser heater was installed to reduce the microbunching instability [14]. The laser heater minimizes the microbunching instability growth by controlling the uncorrelated energy spread of the electron beam. In our experiments, the IR laser beam-size was fixed and the IR laser energy of the laser heater was changed from 0 μJ to 40 μJ by using a half-wave plate. Figure 4 shows the measurement result of the IR laser energy with different angles of the half-wave plate. Figure 5 shows CCD camera images when the laser heater is on and off. The L0, the L1, and the L2 phase are 0°, −11°, and −21°, respectively. The visible radiation intensity is changed with the different IR laser energy. In addition, we also measured the pyroelectric detector intensity with the same IR laser energy. The CSR intensity is decreased as the IR laser energy is increased while the pyroelectric detector intensity does not show any change. This means that the CSR can be used for a monitor of the microbunching instability. After the bunch compressor, the electron beam can produce coherent radiation when the bunch length is shorter than the radiation wavelength. In addition, if the length of the structure, such as the microbunching, in the electron beam is shorter than the radiation wavelength, one can obtain coherent radiation with a strong intensity [15].

SUMMARY

In PAL-XFEL, the CRMs are installed after the bunch compressors for the bunch length measurement. However, a saturation problem was noticed in the pyroelectric detector of the CRM when the bunch length is near to the minimum. To solve the problem, a CCD camera was installed in the CRM chamber, and surprisingly strong radiation was noticed in the visible wavelength with the CCD camera. This strong radiation indicated that the microbunching happened in the electron bunch and it was confirmed from the measurement result with the laser heater.

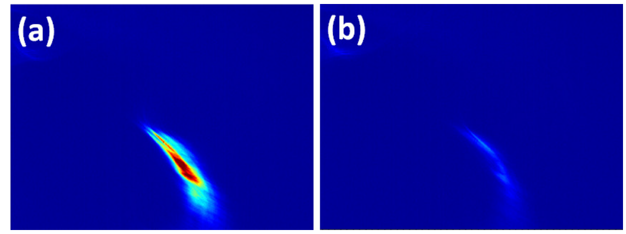

Figure 5: Images of the CCD camera when IR laser energies of the laser heater are (a) 0.55 μJ, (b) 23.6 μJ.

REFERENCES

[1] J. Madey, J. Appl. Phys. **42**, 1906 (1971).

[2] A.M. Kondratenko and E.L. Saldin, Part. Accel. **10**, 1980 (1980).

[3] R. Bonifacio, C. Pellegrini, and L.M. Narducci, Opt. Commun. **50**, 373 (1984).

[4] J. Feldhaus, E.L. Saldin, et al., Nucl. Instrum. Methods Phys. Res. Sect. A **393**, 162 (1997).

[5] E.L. Saldin, E.A. Schneidmiller, M.V. Yurkov, Optics Communications **212**, 377 (2002).

[6] J.B. Rosenzweig, D. Alesini, et al., Nucl. Instrum. Methods Phys. Res. Sect. A **593**, 39 (2008).

[7] The LCLS Design Study Group, SLAC Report No. SLAC-R-521, 1998.

[8] T. Limberg, P. Piot, and E.A. Schneidmiller, Nucl. Instrum. Methods Phys. Res. Sect. A **475**, 353 (2001).

[9] E. L. Saldin, E. A. Schneidmiller, and M.V. Yurkov, Nucl. Instrum. Methods Phys. Res. Sect. A **483**, 516 (2002).

[10] H.-S. Kang et al., Nat. Photon. **11**, 708 (2017).

[11] J. Wu, P. Emma, in Proceedings of LINAC2006 (Knoxville, Tennessee, USA, 2006), 277.

[12] H. Loos, T. Borden, et al., in Proceedings of PAC2007 (New Maxico, USA, 2007), 4189.

[13] J.H. Ko et al., Rev. Sci. Instrum., **89**, 063302 (2018)

[14] J.H. Lee, J.H. Han, et al., Nucl. Instrum. Methods Phys. Res. Sect. A **843**, 39 (2017).

[15] C.J. Hirschmugl, M. Sagurton and G.P. Williams, Phys. Rev. A **44**, 1316 (1991).